Passively Modelocked All-PM Thulium-Doped Fiber Laser at 2.07 μm

Christian Cuadrado-Laborde, José Luis Cruz, Antonio Díez, and Miguel V. Andrés, *Senior Member, IEEE*

***Abstract*—Here we present a self-started passively mode-locked thulium-doped fiber laser with in-band pumping at 1561 nm that fully retains polarization and emits beyond 2 μm. We obtained a sequence of light pulses at 13.084 MHz, where the pulse and spectral widths were 94 ps and 70 pm, respectively, at 2069.5 nm. The measured instantaneous angular frequency shows that these light pulses are chirp-free.**

***Index Terms*—Fiber laser, passive mode-locking, thulium.**

I. Introduction

THERE is a strong motivation to develop reliable oscillators with emission wavelengths at 2 μm and beyond, as they could be used in free-space optical communication [1], low-latency hollow-core fiber interconnection [2], cutting/engraving/welding of plastics [3], laser scalpels [4], eye-safe light detection and ranging (LIDAR) [5], remote sensing [6], real-time spectroscopy [7], optical biopsy [8], etc. Generally, fiber lasers operating around 2 μm can be realized with thulium-doped fibers (TDF) or holmium-doped fibers (HDF) as medium gain [9]. Just below 2 μm, TDF is a natural choice, since the emission cross-section has a maximum centered at 1.85 μm [10]. In contrast, slightly above 2 μm, HDF is the natural candidate for gain medium, since its emission cross-section presents two well-defined peaks centered around 2 μm [11]. Despite this natural predisposition to use HDF as a medium gain above 2 μm there are other reasons of a practical nature to prefer TDFs. One of them is the easier availability of pumping sources for TDFs, which can be pumped at 0.79 or 1.56 μm [9], while HDFs require fewer available pumping sources at 1.1 or 1.9 μm [12]. Another reason is the strong overlap between the emission and absorption bands in HDFs, which promotes re-absorption [9].

The advantages of all-fiber lasers are well known. Especially in the field of all-fiber mode-locking technology with TDF as medium gain, some works with emission wavelengths beyond 2 μm have been presented so far [13]–[21]. However, the commercial introduction of model-locked fiber lasers is hampered by their sensitivity to external disturbances. Thermal and mechanical stresses, ubiquitous in these environments, are known to affect the birefringence properties of fiber cavities, which can lead to unpredictable degradation of device performance. One successful way to minimize this is to construct the resonator using only polarization-maintaining (PM) fibers and components. The proposals presented so far have all been non-polarization preserving, except for [19]. Moreover, all these works are based on indirect pumping into the $^3F_4$ energy level (peak absorption at 790 nm), while the much better efficiency of direct in-band pumping into the $^3H_4$ energy level has been recognized for near-optimal performance (peak absorption at 1610 nm) [22].

In this work, we developed a passive mode-locking thulium-doped fiber laser composed entirely of polarization-maintaining fibers and components. We used a Fabry-Perot resonator defined by the presence of a semiconductor saturable absorber mirror (SESAM) and a highly reflective fiber Bragg grating at both ends. Due to its superior efficiency, we preferred in-band pumping of the TDF at 1561 nm with an all-fiber CW laser. Thus, we obtained a train of light pulses at 13.084 MHz, where the pulse and spectral widths were 94 ps and 70 pm, respectively, at 2069.5 nm. The measured instantaneous angular frequency shows that these light pulses are free of chirp immediately at the output of the resonator. In the following, we first described the experimental setup, and then we experimentally characterized the performance of this laser. Finally, we compare our results with previous works.

II. Experimental Setup

We show in Fig. 1(a) the experimental setup. The resonator is pumped by a CW laser emitting at 1561 nm, with a maximum power of 820 mW; which is in turn pumped with a high-power laser diode emitting at 976 nm (maximum output power of 7.7 W). Therefore, the slope efficiency for the pump unit was $10.57 \pm 0.08\%$, with a lasing threshold of 47 mW. The oscillator consisted of a Fabry-Perot resonator (FP); see Fig. 1(a). The pump unit provides CW light at 1561 nm. which entered the FP cavity via a 99% reflective PM fiber Bragg grating (FBG, $\lambda_B = 2069$ nm and 140 pm bandwidth at –3 dB). Fig. 1(b) shows the measured PM FBG reflectance measured by illuminating the PM FBG with unpolarized light (a 2 μm amplified spontaneous emission light source). Under these conditions,

Manuscript received June 8, 2022; accepted June 15, 2022. Date of publication June 17, 2022; date of current version July 8, 2022. This work was supported in part by the European Union through IPN-Bio project under Grant H2020-MSCA-RISE-2019-872049, and in part by the Generalitat Valenciana of Spain under Grant PROMETEO/2019/048.The work of C. Cuadrado-Laborde was supported by the project CONICET, Argentina, under Grant PIP 2015-0607. *(Corresponding author: Christian Cuadrado-Laborde.)*

Christian Cuadrado-Laborde is with the Instituto de Física Rosario (CONICET-UNR), S2000EZP Rosario, Argentina (e-mail: christian.cuadrado@uv.es).

José Luis Cruz, Antonio Díez, and Miguel V. Andrés are with the Departamento de Fisica Aplicada, Universidad de Valencia, 46100 Burjassot, Valencia, Spain (e-mail: jose.l.cruz@uv.es; antonio.diez@uv.es; miguel.andres@uv.es).

Digital Object Identifier 10.1109/JPHOT.2022.3184071

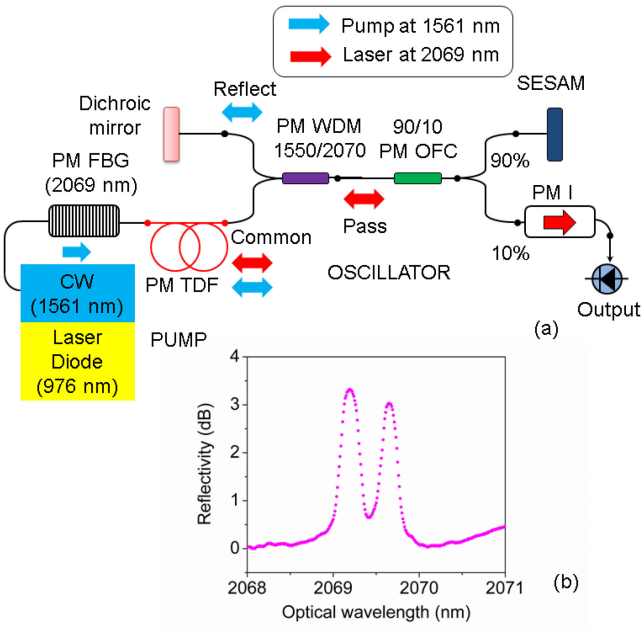

Fig. 1. (a) Experimental setup. (b) Measured reflectivity of the PM FBG.

the measured reflectivity typically shows both reflectance peaks corresponding to the slow and fast axes. However, this is only a consequence of measuring the reflectance with an unpolarized light source, as the reflectance is considerably higher. The PM FBG was fusion-spliced to a 3.2 m PM TDF (PM-TSF 9/125 from Nufern, numerical aperture 0.15, cutoff wavelength 1750 nm, and 9 ± 2 dB/m absorption at 1180 nm). The PM TDF was in turn fusion-spliced to the common port of a PM wavelength division multiplexer (WDM, 1550/2070 nm, insertion loss: pass to common $<$ 0.6 dB at 2070 nm and reflection to common $<$ 0.5 dB at 1550 nm). The reflection port was in turn connected to a dichroic mirror to return to the cavity any residual pump power; while the pass port was connected to the input port of a PM fiber optic coupler (PM OFC, 90/10, central wavelength 1950 nm and fast axis blocked). Finally, a SESAM (BATOP, high reflection bandwidth in the 1900-2080 nm range, and relaxation time constant 10 ps) was mounted on the FC/PC connector of the 90% port of the PM OFC. The output was obtained from the remaining 10% port of the PM OFC, where a PM optical isolator was inserted (PM I, central wavelength of 1950 ± 20 nm, and peak isolation of 28 dB, and insertion loss of 0.6 dB), to avoid unwanted reflections at the cavity. It should be noted that the inclusion of a PM WDM in the setup shown in Fig. 1(a) is not strictly necessary since the pump power at 1561 nm easily reaches the PM TDF via the PM FBG, since the latter is tuned to 2069 nm. However, we decided to include it, otherwise the remaining pump power could reach the SESAM and affect its performance. Simultaneously, we take advantage of this inclusion by reinjecting the remaining pump power present in the cavity using a dichroic mirror. The laser was characterized using a sampling oscilloscope (63 GHz bandwidth), a real-time oscilloscope (13 GHz bandwidth), fast InGaAs photodetectors (rise/fall times $<$ 28 ps), an optical spectrum analyzer (resolution $\geq$50 pm), a 10 GHz electrical spectrum analyzer (resolution $\geq$1 Hz), and finally the average output power was measured with a pyroelectric sensor.

The resulting cavity length is 7.89 m (measured from the PM FBG to the SESAM), with an estimated group velocity dispersion (GVD) of –100 ps^2/km at 2069 nm [23]; i.e., strongly anomalous. The total dispersion for the resonator results in -1.58 ps^2 for roundtrip. Losses in the fiber cavity can be divided into discrete and distributed. The discrete losses are: 0.4 dB (SESAM), 1.49 dB (PM OFC, 90% port), 0.78 dB (PM WDM); i.e., 5.3 dB. On the other hand, the distributed power loss is 40 dB/km; due to the presence of PM 1550 XP and PM TDF (@ 2070 nm). Therefore, the total cavity loss is $\sim$6 dB (per roundtrip).

III. Experimental Results and Discussion

When the 976 nm laser diode power overcomes 2 W, the mode-locked operation self-starts, although with some instabilities. This instability completely disappears when the laser diode pump power reaches the 3 W, i.e., 317 mW of pump power at 1561 nm. At this pump power, the laser delivers a single-pulse train, with a repetition rate of 13.084 MHz; in complete correspondence with the expected roundtrip time for a FP cavity with a full roundtrip length of 15.79 m, see Fig. 2(a). Next, the fast photodetectors were connected to an RF spectrum analyzer. Fig. 2(b) shows the RF traces measured with a resolution bandwidth of 1 Hz for the first harmonic centered at 13.084 MHz; it shows a high extinction sideband suppression ratio of $\sim$80 dB. Fig. 2(c) shows the RF trace measured with a resolution bandwidth of 1 kHz for a wider span covering up to the 7th harmonic. From the RF spectra, we conclude the emission of this laser is very stable, as is evidenced by the absence of any sign of low-frequency instabilities. Further, the use of a SESAM as a mode-locker plus a full polarization-retaining cavity ensures insensitivity against temperature variations and mechanical vibrations.

Fig. 2(d) shows the digital sampling oscilloscope trace for a single light pulse form the output train. The trace can be fitted reasonably well with a sech^2 profile (also shown), and has a full width at half maximum (FWHM) of 94 ps. According to the technical specifications, the photodetector used can measure light pulses with an FWHM of 28 ps $\times$ 2 $\geq$ 56 ps (since the rise and fall times are the same, 28 ps). This proves that the temporal width in Fig. 2(d) is relatively well measured. In addition, it can be observed a small distortion on the falling edge of the pulse waveform, which is probably a consequence of overcompensation to reduce the generally higher fall time of photodetectors [24]. On the other hand, in a previous work, we developed a modelocked TDF laser with a more standard emission wavelength (1951 nm), with a correspondingly lower chromatic dispersion (–1 ps^2); as compared to the actual value of –1.58 ps^2. The output light pulses, in that case, had an FWHM of 81 ps (compared to the actual value of 94 ps) [25]. Since the fundamental repetition rate was approximately the same, they likely have a fairly similar nonlinear parameter; however, the dispersion has increased, resulting in larger pulse width

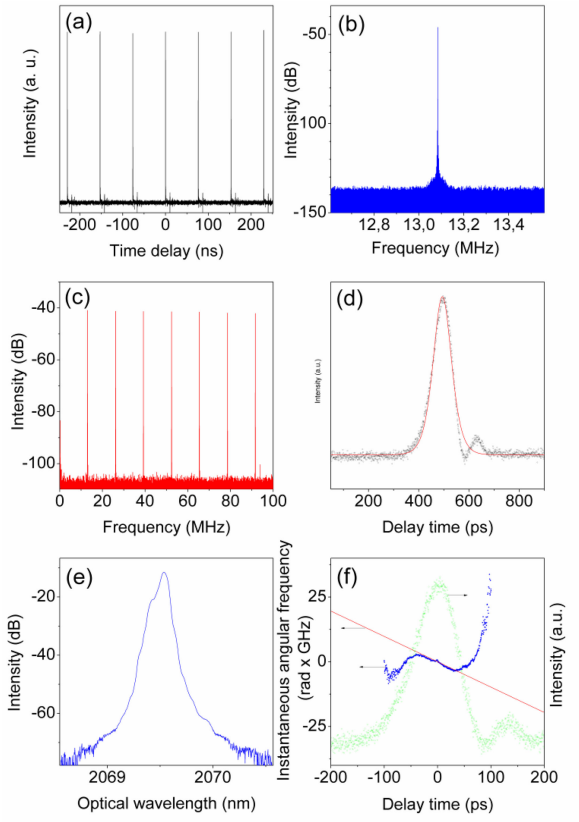

Fig. 2. (a) Pulse train. (b) Electrical spectrum of the first harmonic. (c) the electrical spectrum up to the 7th harmonic. (d) Measured output light pulse with its corresponding sech^2 profile fitting (open dots and solid red curve, respectively). (e) Optical spectra. (f) Instantaneous angular frequency and theoretical chirp (solid blue dots and solid red line, respectively); measured output light pulse (open green dots).

in this case. This result is consistent with previous theoretical studies for soliton lasers where an increase in pulse width is expected with increasing chromatic dispersion for a fixed nonlinear parameter [26], [27]. The average output power measured after the PM isolator with the pyroelectric detector was 0.45 mW. Therefore, the slope efficiency at the output is 0.45 mW/317 mW, or 0.14%. Further, we can estimate an average intracavity power of 10.4 mW, by considering the 90/10 power coupling ratio of the PM OFC and the isolation stage. Since the pulse width is 94 ps, this results in a peak power of 7.94 W with pulse energy of 795 pJ within the resonator.

On the other hand, the optical spectrum is shown in Fig. 2(e). The spectrum has a –3 dB bandwidth of 70 pm at 2069.53 nm. As expected, the bandwidth of the output signal is $\leq$ 140 pm (PM FBG bandwidth), which is the more restrictive filter element in the resonator. Therefore, the obtained time-bandwidth product $TBP = 0.46$; i.e., slightly above a transform-limited sech^2 shape (whose $TBP \geq 0.315$) and close to a transform-limited Gaussian shape (whose $TBP \geq 0.44$) [28]. However, it is well known that solitonic lasers produce transform-limited sech^2 shapes for the output light pulses. Therefore the possibility of a moderately low chirp remains to explain this slight deviation in the *TBP*. For this reason, we followed the procedure developed in Refs.

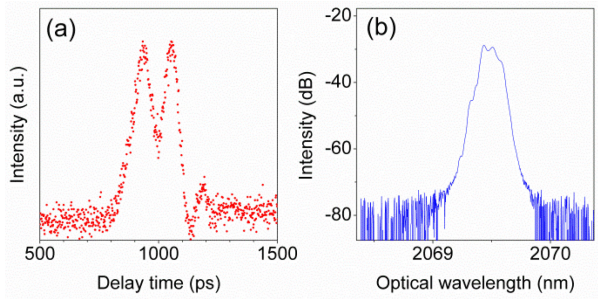

Fig. 3. (a) Measured output light pulses. (b). Optical spectra.

[29], [30] to measure the instantaneous angular frequency. This requires only the measurement of the temporal intensity profiles at the input and output of a given dispersive line of known GVD. For this technique, we used as a dispersive line a 400 m long large effective area fiber (LEAF whose GVD at 2070 nm we estimated to be –102 ps^2/km [31]. Fig. 2(f) shows the obtained profile for the instantaneous angular frequency, showing a moderately low slope compatible with the chirp generated by the length of optical fiber necessary to reach the detectors (6 m) [32]. We, therefore, conclude that these light pulses do not exhibit chirp directly within the resonator. Further, since they are soliton-like pulses, we should mention that the absence of coherent sidebands in the spectrum is related to the strong filtering performed in the resonator by the PM FBG, whose –3 dB bandwidth is only 0.14 nm. This can be confirmed by calculating the wavelength offset of the nearest sidebands, given by $\Delta\lambda = \pm\lambda_0\sqrt{(2/cDL) - 0.0787\lambda_0^2/(c\tau)^2}$, where λ_0 is the central wavelength, c is the speed of light in vacuum, D is the dispersion parameter, and τ is the temporal half-width at half-maximum of the pulse [33]. In the present case, the result is $\Delta\lambda = 6$ nm, which confirms our previous assumption.

When the pump power of the laser diode is increased, the laser enters a multi-pulse region. For example, when the 976 nm laser diode power was increased to 4.1 W, two pulses are generated per roundtrip. Fig. 3(a) shows the digital sampling oscilloscope trace for this dual pulse operation, while Fig. 3(b) shows the optical spectrum. If the pump power is further increased, three pulses per roundtrip appear, and so on until the maximum available pump power of the laser diode is reached. This behavior can be considered typical of soliton lasers. It should also be noted that this regime is not exactly harmonic mode-locking, since the pulses are not evenly distributed over the roundtrip time.

Finally, we have listed in Table 1 a summary of the performance of several modelocked all-fiber lasers with emission wavelengths longer than 2 μm and using TDF as the gain medium (our results have also been included in the last row for simplicity). Compared to these lasers, the mode-locked laser presented in this work has one of the longest emission wavelengths (2070 nm), which is far above the emission maximum at 1837 nm for the $^3F_4 \rightarrow {}^3H_6$ transition. Since the emission cross-section of TDFs covers the range 1650–2200 nm [11]; it might be possible to extend further the wavelength emission of a TDF laser. The reported emission cross-sections, for various TDFs at 2070 nm,

TABLE I
COMPARISON OF THE OUTPUT CHARACTERISTICS OF PREVIOUS TDF MODE-LOCKED ALL-FIBER LASERS WITH EMISSION WAVELENGTHS BEYOND TWO MICRONS*

Reference / Resonator / Mode locker	Pump (nm)	PM	Emission	λ_e (nm)	$\Delta\lambda$ (nm) / ΔT (ps) / TBP
[13]	793	No	Soliton rain	2045	>10
Ring					$>3.6\times10^5$
NPE					$>2.6\times10^5$
[14]	793	No	Gaussian	2020	2.4
Ring					17
Fe-g-CN					2.92
[15]	793	No	DSR	2003	1.7
Ring					2400
SEM/CNT					305
[16]	793	No	DSR	2006	3.4
σ-shaped					1900
					481
[17]	793	No	DS	2010	0.15
Ring					13800
MoS_2					720
[18]	793	No	Soliton-like	2017	1.56
F8					2.8
					0.324
[19]	793	Yes	Soliton-like	2011	10.5
Fabry-Pérot					2.9
SESAM					2.26
[20]	793	No	Noise-like	2048	24.3
Ring					< 1000
NPE					1740
[21]	793	No	DSR	2080	18.3
DBS					>780
					>989
This work	1561	Yes	Soliton-like	2070	0.07
Fabry-Pérot					94
SESAM					0.46

*In this table the following acronyms were used: NPE (nonlinear polarization evolution), Fe-g-CN (iron-doped graphitic carbon nitride), SEM (semiconductor saturable absorber in transmission), CNT (carbon nanotubes), F8 (figure-of-eight), SESAM (semiconductor saturable absorber mirror), DBS (dumbbell-shaped), DS (dissipative solitons), DSR (dissipative soliton resonance).

reaches a maximum of 28% [34], with respect to the maximum value. Therefore, we believe that there are some possibilities of further extending the emission wavelength by using TDFs. The closest emission wavelength is the work reported in [21] with a higher emission wavelength of 2080 nm. However, the output light pulses are very different, as in that case DSR light pulses with giant chirp were obtained, unlike our work where a more standard solitonic output is obtained. Moreover, the output light pulse of this oscillator has the narrowest bandwidth compared to the other works (see Table I). However, it is also true that a broader spectral bandwidth is preferred for some spectroscopy applications, and this design has the potential to enable the generation of a broader emission bandwidth simply by replacing the PM FBG. FBGs with bandwidths up to 0.3 nm can be routinely produced while maintaining the absence of chirp. Finally, this is the first oscillator that provides well-formed chirp-free light pulses in a pure PM configuration beyond 2 μm based on TDF.

IV. CONCLUSION

In this work, we characterized a self-starting passively mode-locked PM-TDFL in-band pumped at 1561 nm. A sequence of 94 ps width light pulses was generated at 13.084 MHz, with a peak power of 7.94 W. The pulses were transform-limited, and their spectral width was 70 pm, centered at 2069.5 nm; which is one of the longest wavelengths reported for solitonic emission based on TDF. These features make this design a promising candidate for various applications, such as in low-latency communications, spectroscopy, LIDAR, and fiber optic sensing.

REFERENCES

[1] P. Lin, T. Wang, W. Ma, Q. Yang, and Z. Liu, "Transmission characteristics of 1.55 and 2.04 μm laser carriers in a simulated smoke channel based on an actively mode-locked fiber laser," *Opt. Exp.*, vol. 28, pp. 39216–39226 2020. [Online]. Available: https://doi.org/10.1364/OE.411743

[2] W. Shen *et al.*, "Low-latency and high-speed hollow-core fiber optical interconnection at 2-micron waveband," *J. Lightw. Technol.*, vol. 38, no. 15, pp. 3874–3882, Aug. 2020. [Online]. Available: https://doi.org/10.1109/JLT.2020.2982971

[3] I. Mingareev, F. Weirauch, A. Olowinsky, L. Shah, P. Kadwani, and M. Richardson, "Welding of polymers using a 2 μm thulium fiber laser," *Opt. Laser Technol.*, vol. 44, pp. 2095–2099, 2012. [Online]. Available: https://doi.org/10.1016/j.optlastec.2012.03.020

[4] X. Xie *et al.*, "A brief review of 2 μm laser scalpel," in *Proc. IEEE 5th Optoelectron. Glob. Conf.*, 2020, pp. 63–67 [Online]. Available: https://doi.org/10.1109/OGC50007.2020.9260447

[5] B.J. Orr, *Infrared LIDAR Applications in Atmospheric Monitoring*. Hoboken, NJ, USA: Wiley, 2017.

[6] C.W. Rudy, M.J.F. Digonnet, and R.L. Byer, "Advances in 2-μm Tm-doped mode-locked fiber lasers," *Opt. Fiber Technol.*, vol. 20, pp. 642–649, 2014. [Online]. Available: https://doi.org/10.1016/j.yofte.2014.06.005

[7] R. Liao, Y. Song, W. Liu, H. Shi, L. Chai, and M. Hu, "Dual-comb spectroscopy with a single free-running thulium-doped fiber laser," *Opt. Exp.*, vol. 26, pp. 11046–11054, 2018. [Online]. Available: https://doi.org/10.1364/OE.26.011046Principio

[8] R. Alfano and Y. Pu, "11 - Optical biopsy for cancer detection," in *Woodhead Publishing Series in Electronic and Optical Materials, Lasers for Medical Applications*, H. Jelínková, Ed., Sawston, U.K.: Woodhead Publishing, 2003, pp. 325–367, [Online]. Available: https://doi.org/10.1533/9780857097545.3.325

[9] R. Cao, Y. Lu, Y. Tian, F. Huang, S. Xu, and J. Zhang, "Spectroscopy of thulium and holmium co-doped silicate glasses," *Opt. Mater. Exp.*, vol. 6, pp. 2252–2263, 2016. [Online]. Available: https://doi.org/10.1364/OME.6.002252

[10] M.A. Khamis and K. Ennser, "Broadband amplified spontaneous emission thulium-doped fiber sources near 2 μm," in *Horizons in World Physics*, vol. 299, A. Reimer, Ed., New York, USA: Nova Science Publishers 2019, chapter 3.

[11] A. Hemming, N. Simakov, J. Haub, and A. Carter, "A review of recent progress in holmium-doped silica fibre sources," *Opt. Fiber Technol.*, vol. 20, pp. 621–630, 2014. [Online]. Available: https://doi.org/10.1016/j.yofte.2014.08.010

[12] J. Lee and J.H. Lee, "A passively Q-switched holmium-doped fiber laser with graphene oxide at 2058 nm," *Appl. Sci.*, vol. 11, 2021, Art. no. 407. [Online]. Available: https://doi.org/10.3390/app11010407

[13] F. Wang, X.-l. Zhang, J.-H. Cui, and J.-J. Huang, "Evolution of soliton rain in a Tm-doped passive mode-locked all-fiber laser," *IEEE Photon. J.*, vol. 12, no. 4, Aug. 2020, Art. no. 1503408, [Online]. Available: https://doi.org/10.1109/JPHOT.2020.3012571

[14] Y. Luo *et al.*, "Mode-locked Tm-doped fiber laser based on iron-doped carbon nitride nanosheets," *Laser Phys. Lett.*, vol. 14, 2017, Art. no. 110002. [Online]. Available: https://doi.org/10.1088/1612-202x/aa7d82

[15] M. Wang, Y. Huang, Z. Song, J. Wei, J. Pei, and S. Ruan, "Two-micron all-fiberized passively mode-locked fiber lasers with high-energy nanosecond pulse," *High Power Laser Sci. Eng.*, vol. 8, 2020, Art. no. 02000e14. [Online]. Available: https://doi.org/10.1017/hpl.2020.7

[16] T. Du, W. Li, Q. Ruan, K. Wang, N. Chen, and Z. Luo, "2 μm high-power dissipative soliton resonance in a compact σ-shaped Tm-doped double-clad fiber laser," *Appl. Phys. Exp.*, vol. 11, 2018, Art. no. 052701. [Online]. Available: http://dx.doi.org/10.7567/APEX.11.052701

[17] X.-F. Wang *et al.*, "2-μm mode-locked nanosecond fiber laser based on MoS_2 saturable absorber," *Chin. Phys. B*, vol. 26, 2017, Art. no. 114205. [Online]. Available: https://doi.org/10.1088/1674-1056/26/11/114205

[18] J. Li *et al.*, "All-fiber passively mode-locked Tm-doped NOLM-based oscillator operating at 2-μm in both soliton and noisy-pulse regimes," *Opt. Exp.*, vol. 22, pp. 7875–7882, 2014. [Online]. Available: https://doi.org/10.1364/OE.22.007875

[19] P. Wan, L.-M. Yang, and J. Liu, "High power 2 μm femtosecond fiber laser," *Opt. Exp.*, vol. 21, pp. 21374–21379, 2013. [Online]. Available: https://doi.org/10.1364/OE.21.021374

[20] X.-F. Wang, Z.-G. Jin, and J.-H. Liu, "2.04 μm harmonic noise-like pulses generation from a mode-locked fiber laser based on nonlinear polarization rotation," *Optoelectron. Lett.*, vol. 17, pp. 18–21, 2021. [Online]. Available: https://doi.org/10.1007/s11801-021-0028-3

[21] H. Wang *et al.*, "2080 nm long-wavelength, high-power dissipative soliton resonance in a dumbbell-shaped thulium-doped fiber laser," *Chin. Opt. Lett.*, vol. 17, 2019, Art. no. 030602. [Online]. Available: http://dx.doi.org/10.3788/COL201917.030602

[22] S.D. Jackson and T.A. King, "Theoretical modeling of Tm-doped silica fiber lasers," *J. Lightw. Technol.*, vol. 17, pp. 948–956, 1999. [Online]. Available: https://doi.org/10.1109/50.762916

[23] A. Rampur *et al.*, "Ultra low-noise coherent supercontinuum amplification and compression below 100 fs in an all-fiber polarization-maintaining thulium fiber amplifier," *Opt. Exp.*, vol. 27, pp. 35041–35051, 2019. [Online]. Available: https://doi.org/10.1364/OE.27.035041

[24] A. Shakoor, K. Nozaki, E. Kuramochi, K. Nishiguchi, A. Shinya, and M. Notomi, "Compact 1D-silicon photonic crystal electro-optic modulator operating with ultra-low switching voltage and energy," *Opt. Exp.*, vol. 22, pp. 28623–28634, 2014. [Online]. Available: https://doi.org/10.1364/OE.22.028623

[25] L.A. Sánchez, C. Cuadrado-Laborde, A. Carrascosa, A. Díez, J.L. Cruz, and M.V. Andrés, "Low-repetition-rate all-polarization maintaining thulium-doped passively modelocked fiber laser," *Opt. Laser Technol.*, vol. 149, 2022, Art. no. 107856. [Online]. Available: https://doi.org/10.1016/j.optlastec.2022.107856

[26] O.E. Martinez, R.L. Fork, and J.P. Gordon, "Theory of passively mode-locked lasers including self-phase modulation and group-velocity dispersion," *Opt. Lett.*, vol. 9, pp. 156–158, 1984. [Online]. Available: https://doi.org/10.1364/OL.9.000156

[27] H.A. Haus, "Mode-locking of lasers," *IEEE J. Sel. Topics Quantum Electron.*, vol. 6, no. 6 pp. 1173–1185, Nov/Dec. 2000. [Online]. Available: https://doi.org/10.1109/2944.902165

[28] A.E. Siegman, *Lasers*. Sausalito, CA, USA: Univ. Science Books, 1986.

[29] C. Cuadrado-Laborde, A. Carrascosa, P. Pérez-Millán, A. Díez, J.L. Cruz, and M.V. Andrés, "Phase recovery by using optical fiber dispersion," *Opt. Lett.*, vol. 39, pp. 598–601, 2014. [Online]. Available: https://doi.org/10.1364/OL.39.000598

[30] C. Cuadrado-Laborde, M. Brotons-Gisbert, G. Serafino, A. Bogoni, P. Pérez-Millán, and M.V. Andrés, "Phase recovery by using optical fiber dispersion and pulse pre-stretching," *Appl. Phys. B*, vol. 117, pp. 1173–1181, 2014. [Online]. Available: https://doi.org/10.1007/s00340-014-5941-8

[31] Product Information of Corning LEAF optical fiber, 2014. [Online]. Available: www.corning.com/media/worldwide/coc/documents/Fiber/LEAF%20optical%20fiber.pdf

[32] G.P Agrawal, *Nonlinear Fiber Optics*, 6th ed., Cambridge, MA, USA: Academic Press, 2019.

[33] M. L. Dennis and I. N. Duling, "Experimental study of sideband generation in femtosecond fiber lasers," *IEEE J. Quantum Electron.*, vol. 30, no. 6, pp. 1469–1477, Jun. 1994. [Online]. Available: https://doi.org/10.1109/3.299472

[34] S. Jackson, "The spectroscopic and energy transfer characteristics of the rare earth ions used for silicate glass fibre lasers operating in the short-wave infrared," *Laser Photon. Rev.* vol. 3, pp. 466–482, 2009. [Online]. Available: https://doi.org/10.1002/lpor.200810058